Published in final edited form as:
Annu Rev Anal Chem (Palo Alto Calif). 2009 July 1; 2: 57–76. doi:10.1146/annurev.anchem.1.031207.112823.

Nanoparticle PEBBLE sensors in live cells and in vivo

Yong-Eun Koo Lee, PhD,
University of Michigan, Department of Chemistry, 930 N. University, Ann Arbor, MI 48109-1055

Raoul Kopelman, PhD, and
University of Michigan, Department of Chemistry, 930 N. University, Ann Arbor, MI 48109-1055

Ron Smith
University of Michigan, Department of Chemistry, 930 N. University, Ann Arbor, MI 48109-1055

Yong-Eun Koo Lee: yeleekoo@umich.edu; Raoul Kopelman: kopelman@umich.edu; Ron Smith: rongsmit@umich.edu

Abstract

Nanoparticle sensors have been developed for imaging and dynamic monitoring, in live cells and in vivo, of the molecular or ionic components, constructs, forces and dynamics, all in real time, during biological/chemical/physical processes. With their biocompatible small size and inert matrix, nanoparticle sensors have been successfully applied for non-invasive real-time measurements of analytes and fields in cells and rodents, with spatial, temporal, physical and chemical resolution. This review describes the diverse designs of nanoparticle sensors for ions and small molecules, physical fields and biological features, as well as the characterization, properties, and applications of these nanosensors to in vitro and in vivo measurements. Their floating as well as localization ability in biological media is captured by the acronym PEBBLE: photonic explorer for bioanalysis with biologically localized embedding.

Keywords

Nano-sensor; ion; molecule; ROS; fluorescence; chemiluminescence; SERS; LSPR; MRI

1. Introduction

An ideal bioanalytical and biomedical sensor should achieve, in live cells and in vivo, real-time tracking of biological/chemical/physical processes as well as detection of disease related abnormal features, with no interferences. Traditional sensors like microelectrode or fiber optical sensors are not even close to the ideal sensor, due to their large size causing physical invasiveness, despite many efforts toward miniaturization (1).

Fluorescent molecular probes have so far been playing a major role for intracellular sensing and imaging (2). Their fast response, intense signal, against relatively low background noise, and the relatively simple instrumental set-up, have made the molecular probe-based fluorescence technique a perfect match for real time measurements in cells. These molecular probes, however, have several drawbacks affecting reliable intracellular measurement (3,4). The probe molecules have to be in a cell permeable form, which often requires proper derivatization of the molecules, which in itself might interfere with their function. The cytotoxicity or perturbed effects of the available dyes is often a problem as the mere presence of these dye molecules may chemically interfere with the cell's processes. The intracellular

Correspondence to: Yong-Eun Koo Lee, yeleekoo@umich.edu; Raoul Kopelman, kopelman@umich.edu.

measurement is often skewed by sequestration to specific organelles inside the cell, or by non-specific binding to proteins and other cell components. Furthermore, the dye is usually not "ratiometric", i.e., has only a single spectral peak, which then requires technologically more demanding techniques, such as picosecond lifetime resolution or phase sensitive detection. It should be noted that just loading into the cell a separate reference dye, for ratiometric measurements, is not a solution, because of the aforementioned sequestration and non-specific binding. The impact of these drawbacks is even more severe for in vivo application. Only a small portion of the molecular probes would reach a specific location of interest within the body, which has also been an issue for drug delivery. The same goes for crossing biological barriers, e.g. the blood-brain-barrier. So has been the issue of multiple drug resistance, caused by the ability of certain tumor cells to pump out small drug, or probe, molecules. Moreover, there is an issue of limited tissue penetration-depth by photons, for in vivo measurements using optical methods. For deep tissue imaging (millimeters to centimeters), it is necessary to use near-infrared (NIR) light in the spectral range of 650–900 nm, which is separated from the major absorption peaks of blood and water (5–7). The NIR region is free from autofluorescence of cellular components and therefore advantageous for intracellular measurements, too. We note that most of the currently available molecular probes have visible absorption/emission wavelength. Nanoparticle probes can be easily tailored for the NIR spectral range.

Advances in nanotechnology have made many types of nanoparticles available as platforms for constructing new types of bioanalytical sensors. The nanoparticles are in the dimension range of 1–1000 nm, i.e. from a few atoms to mitochondria size, thus resulting in minimal physical interference to cells. For example, a single spherical nanoparticle of 500 nm in diameter is at least four orders of magnitude smaller in volume than a typical mammalian cell (8), and a 20 nm particle is eight orders of magnitude smaller, thus minimizing interference due to physical size. Most of the nanoparticle matrices are non-toxic and therefore the nanoparticles do not cause chemical interference to cells, either. The delivery of nanoparticles into cells or animals can be done by standard delivery methods. The intracellular delivery methods of nanoparticles, through the plasma membrane barrier, include pico injection; gene gun delivery (9,10); liposome incorporation (11); non-specific or receptor-mediated endocytosis with surface conjugated translocating proteins/peptides (12–14); and membrane penetrating TAT peptides (15,16) (Figure 1). We note that there is negligible physical and chemical perturbation to the cell by these delivery techniques. For example, cell viability after gene gun delivery was found to be about 99% compared to control cells (11). Once delivered into cells, these sensors can be used with conventional microscopy techniques, enabling high spatial and temporal resolution. Intravenous injection is a typical method of in vivo delivery of the nanoparticles.

Nanoparticles have many advantages (4,17), as building blocks for intracellular or in vivo sensors due to their non-toxicity and excellent engineerability: 1) The inert matrix protects cellular contents from the incorporated sensing components and *vice versa*. The nanoparticle matrix eliminates interferences such as protein binding and/or membrane/organelle sequestration. 2) Each nanoparticle can be loaded with a high amount of sensing components due to the larger size of the nanoparticle compared to the molecular dyes, enhancing the ratio of signal/background. 3) Loading of multiple components per each nanoparticle is also possible, allowing ratiomentric measurements as well as multiplex sensing or sophisticated synergistic designs. The ratiometric mode of operation assures that the measurements will be unaffected by excitation intensity, absolute concentration and sources of optical loss, which is essential for intensity-based intracellular or *in vivo* measurement where there are many interfering factors. 4) Nanoparticles can be surface-coated with biological molecules like proteins and peptides for targeting to specific cells or designing sensors (18), or with polyethylene glycol (PEG) for reduced non-specific binding and longer plasma half-life. Such surface-modification is especially useful for in vivo sensing as it will help increase the

accumulation of the nanoparticles at the location of interest. 5) Nanoparticles have a high surface-to-volume ratio, resulting in high accessibility of analytes/targets to the indicator-dyes/receptors. In some cases, high loaded amounts of dyes in close proximity to each other, either within the nanoparticle matrix or on its surface, can allow multiple interactions with the sensing components, resulting in signal amplification (19). It is noteworthy that similar amplification effects have been reported for the targeting efficiency of nanoparticle with multiple surface-conjugated targeting moieties (20). 6) Some types of nanoparticles possess unique but controllable optical/magnetic properties which are superior to molecular probes. For example, semiconductor nanoparticles, commonly called quantum dots (QDs), have large fluorescence quantum yields, resistance to photobleaching and good chemical stability. The optical properties of QDs are tunable by controlling the size, composition and preparation procedures. Metallic nanoparticles (Metal nanoparticle or metal nanoshell coated on polymer nanoparticle) have localized surface plasmon resonance (LSPR) and induce surface-enhanced Raman scattering (SERS), which are free from photobleaching (21). The LSPR wavelength of the metallic nanoparticles can be tuned by changing the shape, size and composition of the metal nanoparticle or metal shell thickness (22,23). Superparamagnetic iron oxides (SPIOs) provide negative contrast enhancement for MRI. These characteristics can be utilized for constructing various multiplex sensors.

A wide variety of nanoparticle sensors have been reported since the first of a kind nanoparticle sensors, so called nano-PEBBLE (Photonic Explorer for Biomedical use with Biologically Localized Embedding) by Kopelman and colleagues over a decade ago (24,25).

Some of the nanoparticle sensors have been developed for intracellular or in vivo measurements of metabolites such as ions and small molecules and cell-related processes/forces. Some of them have been developed for large molecules such as proteins or nucleic acids, which are mainly for laboratory diagnostic assay in body fluids or tissues. We note that the same nanoparticle platform concept has been extended to design a nano medical device, i.e., by loading the nanoparticle with contrast imaging agents and/or therapeutic agents, instead of sensing elements (17,26,27), i.e., nano-theranostic devices. The in vivo application of the medical nanoparticle device has been quite successful in cancer imaging and therapy (14,17, 28), aided by an EPR (Enhanced Permeability and Retention) effect (29) which allows preferential accumulation at tumor sites due to the “size” advantages of nanoparticles. The nanodevice showed an enhanced targeting efficiency when it is surface-conjugated with targeting moieties specific to the overly expressed proteins in tumor cells or vasculatures (14,30,31). These bio-conjugated nanoparticles for cancer detection may also be called sensors but will not be covered here.

This review focuses on the design, properties and applications of nanoparticle-based bioanalytical sensors for small molecules and ions, aiming at in situ measurements in live cells and in vivo. The nanoparticle sensors for large molecules will not be covered as they have been developed mainly for laboratory diagnosis assay (32–35). Mechanically fixed nanosensors like fiber-tip had historical contributions to live cell sensing (36) but are little used now. Film on glass slide or microarray on a chip sensors are rarely suitable for intracellular or in vivo measurements and therefore will not be covered here, even when they utilize nanoparticles.

2. Nanoparticle sensors: Design and Preparation

A typical design of nanoparticle sensors uses the nanoparticle as a chemically inert platform, loaded with sensing components. The sensing mechanism involves the permeation of analytes into the nanoparticle matrix and their selective interaction with sensing components, resulting in signal changes. The important properties of sensors, such as sensitivity, dynamic range, selectivity, reversibility and stability, mostly depend on the incorporated sensing components.

However, the nanoparticle matrix also plays an important role; the properties of the matrix, such as pore size, hydrophobicity and charge, do determine the permeability and solubility of the analytes, as well as the loading efficiency of the sensing probes (4). For example, polyacrylamide (PAA) nanoparticles have served as a good matrix for ion sensors (37–41), due to their neutral and hydrophilic nature, while a hydrophobic nanoparticle matrix is preferred for oxygen sensors (10,42). A wide variety of nanoparticle matrices have been used as sensor platforms, which includes polymer nanoparticles made of organic, inorganic, or organic-inorganic hybrid materials, polymer-capped liposomes or micelles, semiconductor nanoparticles, as well as metallic (metal or metal shell) nanoparticles. We note that the pores of the nanoparticle matrix are sufficiently large to allow diffusion of the smaller analyte ions or molecules, so as to bind with molecular probes located inside the nanoparticle, but the pores are still small enough to exclude the diffusion of larger proteins into the core matrix. This exclusion of macromolecules is quite significant, since many “naked molecule” dyes change their fluorescence properties in the presence of proteins. On the other hand, the nanoparticle sensors containing the very same dyes were found not to be affected by protein presence (37, 39,42,43). The sensing components typically include indicator and reference dyes, or a combination of reporter dyes and analyte-specific ligands, or biological receptors. Loading of the sensing components into the nanoparticles is made during synthesis, or after the formation of the nanoparticles, by encapsulation, covalent linkage, bio-affinity interaction such as streptavidine-biotin, or physical adsorption through charge-charge or hydrophobic interaction. The covalent linkage is typically made by simple coupling reactions between the nanoparticle functionalized with amine-, carboxyl- or thiol- groups and the molecules containing similar functional groups. Biological molecules such as antibodies, DNAs and peptides have been used as receptors due to their highly selective biological interactions. These biomolecular receptors have also been utilized as targeting moieties, which enables nanoparticles to perform real-time tracking of target biomolecules in cells (15) as well as tumor-targeted delivery of drugs or image contrast agents in rodents (14,17) If targeting moieties are added to the nanoparticle sensors, the sensors can even detect or sense specific analytes in a spatially localized target area (44).

QDs, metallic nanoparticles and SPIOs have been used as part of a sensing core as well as a platform. The optical or magnetic characteristics of these nanoparticles do not themselves change in response to specific analytes. These characteristics, however, can change in response to specific analytes when these nanoparticles are labeled with suitable dyes, ligands or receptors.

Figures 2 and 3 show the kinds of nanoparticle sensors that have been designed so far. Most nanoparticle sensors use fluorescence (Figures 2a, 2b, 2d, 2e, 2f) and Figure 3a) as a detection signal but some use chemiluminescence (Figure 2c), scattering (Figures 3b and c), absorbance (Figure 3c) or magnetic resonance (Figure 3c). The properties and in vitro and in vivo applications of each type of nanoparticle sensor are detailed in the section below.

3. Nanoparticle sensors: properties and applications

3.1 Polymer nanoparticle sensors with fluorescent indicator dyes

In this design (Figure 2a), the fluorescent indicator and reference dyes are loaded into the polymeric nanoparticle core or its surface coated layer and there is no interaction between the dyes. The nanoparticle sensors based on this design have been developed to sense ions (H^+, Ca^{2+}, Mg^{2+}, Zn^{2+}, Fe^{3+}, K+) (11, 37–41, 45, 46), radicals (OH radical) (47), small molecules (O_2, singlet oxygen, hydrogen peroxide) (10, 42, 48–53, 54) as well as cellular electric field (55).

Ion sensors—Most ion nanoparticle sensors under this category are the PEBBLE sensors, which are made of hydrophilic PAA nanoparticles with encapsulated fluorescent dyes. However, there are a few reports on different designs. For example, a pH nanoparticle sensor was prepared using the PAA nanoparticle with covalent linked dyes (45) and a K^+ nanoparticle sensor by loading the sensing dye into the surface coated layer polyelectrolytes instead of the nanoparticle itself (46). Successful intracellular measurements have been demonstrated by the PEEBLE sensors for pH, Mg^{+2} and Ca^{2+} (11,24,37,38). The Mg^{2+} PEBBLE sensor is an interesting example in terms of design and cellular application. It achieved both high selectivity and sensitivity by using the right combination of nanoparticle matrix and dyes. The traditional measurement of magnesium ion concentrations in biological environments has suffered from severe interference due to calcium ions. Coumarine 343 is a small hydrophilic dye that does not penetrate the cell membrane by itself but is a very sensitive Mg^{2+} ion probe, which has a higher selectivity for magnesium over calcium than any commercially available probe. The Mg^{2+} PEBBLE sensor was constructed by encapsulating this hydrophilic dye and a commercial reference dye ("Texas Red") in a hydrophilic PAA nanoparticle (37). The linear response of these PEBBLEs to Mg^{2+} ion, in the range of 0.1 – 10 mM, is not interfered with even in the presence of, simultaneously, 1 mM calcium, 20 mM sodium and 120 mM potassium, demonstrating thereby that this Mg^{2+} PEBBLE should serve as a reliable indicator of intracellular Mg^{2+} concentrations. These Mg^{2+} PEBBLEs were indeed utilized to determine the role of Mg^{2+} inside human macrophage cells in the presence of invading salmonella bacteria (56). The Mg^{2+} measurements by the PEBBLE sensors showed conclusively that Mg^{2+} is not an important contributor in the control of pathogens by macrophages, in contradiction to previous reports (57).

Dissolved Oxygen Sensor—The first nanoparticle sensor for dissolved oxygen was the silica-based PEBBLE sensor which was prepared by embedding $[Ru(dpp)_3]^{2+}$, i.e. ruthenium oxygen indicator dyes, as well as reference dyes into silica nanoparticles (49). The sensor was applied successfully for reliable intracellular oxygen imaging in live C6 glioma cells (Figure 4). Oxygen PEBBLE sensors with enhanced sensitivity and dynamic range were developed using the more sensitive platinum-based oxygen dyes, as well as reference dyes, embedded in a hydrophobic matrix, such as organically modified silica (ormosil) (10) or PDMA (42). The hydrophobic matrix is usually better suited for oxygen sensing than the hydrophilic one due to the higher oxygen solubility in it. These hydrophobic PEBBLE nanosensors exhibit a perfectly linear Stern-Volmer calibration curve over the entire range of dissolved oxygen concentrations, an ideal but previously unachieved goal for any fluorescent oxygen sensors. The sensitivity, represented by Q_{DO}, was 97–97.5%, which is the highest among the reported values. Q_{DO} is the quenching response to dissolved oxygen, defined by

$$Q_{DO}=(I_{N_2}-I_{O_2})/I_{N_2}\times 100$$

where I_{N_2} is the fluorescence intensity of the indicator dye or the indicator/reference intensity 2 ratio, in fully deoxygenated water, and I_{O_2} is that in fully oxygenated water.

The embedded platinum(II) octaethylporphine ketone, another oxygen-sensitive dye, has infrared fluorescence and makes such sensors workable even in human plasma samples (42), unaffected by the plasma's notoriously high light scattering and autofluorescence. The oxygen PEBBLE sensors made of ormosil nanoparticles were successfully applied for real-time imaging of oxygen inside live cells, i.e. monitoring metabolic changes inside live C6 Glioma cells (10).

Oxygen sensors have also been developed by embedding the ruthenium dyes into the polyelectrolyte layers on commercial fluorescent nanoparticle surfaces (50) or into polymerized phospholipid vesicles (liposomes) (51). However, the sensitivities of these sensors were only 60% for polyelectrolyte coated nanoparticle sensors and 76% for polymerized liposome sensors.

The oxygen measurements above are all based on fluorescence intensity. Other methods such as fluorescence anisotropy (43) and life-time measurement (52,53) have been also utilized. For example, the oxygen concentration inside green plant cells was measured with the nanoparticle sensors injected by glass micro-capillaries. The sensors were constructed by encapsulating Pt (II)-tetra-pentafluorophenyl-porphyrin (PtPFPP) in polystyrene beads of 0.3–1um in diameter (52). The same sensors were injected into the salivary glands of the blowfly to quantify the changes in oxygen content within individual gland tubules during hormone-induced secretory activity (53). The nanoparticle sensors for dissolved oxygen are summarized in Table 1.

Sensors for Reactive Oxygen Species (ROS)—Ratiometric PEBBLE sensors were developed for ROS, singlet oxygen, hydrogen peroxide and hydroxyl radical, using irreversible molecular probes. A singlet oxygen PEBBLE sensor was prepared by incorporating the singlet-oxygen–sensitive 9,10-dimethyl anthracene or the singlet-oxygen–insensitive octaethylporphine within ormosil nanoparticles (48). The nanoparticle matrix enhances the selectivity of the indicator dye toward singlet oxygen as the matrix blocks the entry of short-lived polar ROS, such as OH and superoxide radicals. These nanoprobes have been used to monitor the singlet oxygen produced by “dynamic nanoplatforms” that were developed for photodynamic therapy (14). Another singlet oxygen PEBBLE sensor was constructed with ormosil nanoparticles incorporated with 1,3-diphenylisobenzofuran (DPIBF). The intracellular concentration of singlet oxygen within C6 glioma cells during PDT was measured with the DPIBF sensors (54). A PEBBLE sensor for hydrogen peroxide (H_2O_2) was prepared by embedding 2′,7′-dichlorofluorescine diacetate into ormosil nanoparticles. The PEBBLE sensors did successfully detect H_2O_2 within macrophage in low nM concentration (54).

A PEBBLE sensor for OH radical was designed by covalently attaching the hydroxyl indicator dye, coumarin-3-carboxylic acid, onto the PAA nanoparticle surface, while encapsulating the reference dye deep inside it (47). This design circumvents two potential problems from the hydroxyl radical, the most reactive ROS: 1. Inability to penetrate significantly into any matrix without being destroyed; 2. Ability to oxidize (and photobleach) most potential reference dyes. This nano-probe demonstrates a proof of principle of a ratiometric hydroxyl radical probe, with good sensitivity and reversibility.

Nanoparticle sensors for electric field—A nano-sensor, called E-PEBBLE, was developed by encasing the fast response, voltage sensitive fluorescent dye di-4-ANEPPS inside silane capped (polymerized) micelles (55). The hydrophobic core of the micelle provides a uniform environment for the molecules and therefore allows for universal calibration. It also allows for fast orientation of these dye molecules, which shortens the response time. The E-PEBBLEs were introduced into DITNC astrocytes by endocytosis and enabled, for the first time, complete 3-dimensional electric field profiling throughout the entire volume of living cells (not just inside membranes) (Figure 5). It is to be noted that traditional methods like free voltage dyes or patch/voltage clamps require calibration steps for each cell or cell type measured and the measurements are confined to the cellular membranes, which are only 0.01% of the cell volume. This new ability is expected to greatly enhance the understanding of the role of cellular E fields in influencing and/or regulating biological processes, with wider implications for cellular biology, biophysics, biochemistry and medicine.

3.2 Ion-correlation nanoparticle sensors

In this design of ion sensing nanoparticle sensors (Figure 2b), the hydrophobic polymeric nanoparticle is loaded with three lipophilic components: a highly selective but optically silent ionophore, a pH sensitive fluorescent dye, and an ionic additive. The ion-correlation nanoparticle sensors have been developed for K^+, Na^+, and Cl^- ions (9, 58–62). The ion sensing is based on the same mechanism as that for fluorescent ion selective optodes (63–66). When a selective ionophore binds the ions of interest, thermodynamic equilibrium-based ion exchange (for sensing cations) or ion coextraction (for sensing anions) occurs simultaneously. This changes the local pH in proportion to the concentration of the ion of interest within the nanoparticle matrix, which is optically detected by the pH-sensitive dye. The ionic additive is used to maintain ionic strength. We note that in a modified design (61), the ions are measured by bright fluorescence of QDs instead of pH dye, utilizing the overlap of the emission of the embedded QDs with the absorbance of the pH dye. The hydrophobic nanoparticle matrixes for the ion-correlation sensors include polydecylmethacrylate (PDMA) (9, 58, 59), poly n-butyl acrylate (PnBA) (62) and poly(vinyl chloride) (PVC) (60, 61). The composition of the matrix as well as the ratios of the three sensor components were found to affect the sensor characteristics such as dynamic range, selectivity and response time (9, 62). The ion-correlation nanoparticle sensors are very sensitive and selective. For example, the sensitivity of the two K^+ ion-correlation nanoparticle sensors is higher by a factor of 1,000–10,000 than that of the K^+ nanoparticle described in section 3.1 above (46). Intracellular measurements have been made for K^+, Na^+ and Cl^- using PDMA based PEBBLE sensors. For example, the PDMA K^+ PEBBLE sensors were gene-gun delivered into rat C6 glioma cells and successfully measured an increase in the intracellular K^+ concentration after adding kainic acid, a K^+ channel opening agonist (9).

3.3 Chemiluminescence nanoparticle sensors

Chemiluminescence was utilized to design sensors for hydrogen peroxide (Figure 2c) (67). The sensor was made of peroxalate ester nanoparticles and encapsulated fluorescent dyes. The sensing mechanism is as follows: hydrogen peroxide reacts with the peroxalate ester groups, generating a high-energy dioxetanedione, which then chemically excites encapsulated fluorescent dyes, leading to chemiluminescence. The sensor has nanomolar sensitivity for hydrogen peroxide and excellent specificity for hydrogen peroxide over other ROS. The chemiluminescence wavelength was tunable by changing the encapsulated fluorescent dyes. For example, the peroxalate particles containing perylene, rubrene and pentacene emitted light at wavelengths of 460, 560 and 630 nm, respectively. The nanoparticle sensors with encapsulated pentacene were applied for in vivo imaging of hydrogen peroxide, externally injected as well as endogenously produced in the peritoneal cavity of mice during lipopolysaccharide -induced inflammatory response (67).

3.4 Polymer nanoparticle sensors with encapsulated protein

Two types of nanosensors operating on different sensing mechanisms have been developed with this design (Figure 2d). In the first type, the encapsulated protein behaves as a fluorescent molecular probe. The nanoparticle sensors for copper and phosphate ions are two examples. The $Cu^{+/2+}$ sensor was constructed by incorporating DsRed, red fluorescent protein and a reference dye in PAA nanoparticles (40). The detection range for Cu^+ and Cu^{2+} was 0.2–5 μM. The phosphate sensor was made of PAA nanoparticles and embedded fluorescent phosphate sensing proteins, (FLIPPi), with μM detection range (68). In the second type, the encapsulated protein is an enzyme which catalyzes the reaction involved with analytes. The enzymatic reaction leads to fluorescence change either by fluorescence product or by co-embedded fluorescent indicator dye for depleted reactant. Examples include a glucose sensor and two hydrogen peroxide sensors. The glucose sensor was developed by incorporating

glucose oxidase (GO_x), an oxygen sensitive ruthenium-based dye, and a reference dye within PAA nanoparticles (69). The enzymatic oxidation of glucose to gluconic acid results in the local depletion of oxygen, which increases the fluorescence of the encapsulated oxygen sensitive dye. The dynamic range was found to be ~ 0.3–8 mM, which is suitable for intracellular measurements. The hydrogen peroxide nanoparticle sensors were developed by encapsulating horseradish peroxidase (HRP) within either PAA (70) or PEG (71) nanoparticles. The PAA-based sensor has co-embedded fluorescein dye, the fluorescence intensity of which decreases when HRP catalyzes the oxidation of dye in the presence of ROS (70). The PEG-based sensor uses externally introduced Amplex Red (10-acetyl-3,7-dihydroxyphenoxazine) for H_2O_2 meassurement (71). The encapsulated HRP catalyzes the reaction between Amplex Red and H_2O_2, forming red fluorescent product, resorufin, in proportion to the amount of H_2O_2. The sensors were phagocytized into macrophages, responded to exogenous H_2O_2 (100 μM) as well as endogenous peroxide induced by lipopolysaccharide (1 μg/mL).

3.5 FRET-based nanoparticle sensors

The sensor based on Fluorescence Resonance Energy Transfer (FRET) mechanism is typically designed in three ways: 1) polymer nanoparticles loaded with an analyte-insensitive fluorescent dye and analyte-selective molecules or ligands (Figure 2e); 2) QDs with surface-conjugated analyte-selective molecules or ligands (Figure 2f); 3) metallic nanoparticles with surface-conjugated analyte-selective fluorescent molecules or ligands (Figure 3a). Here, the metallic nanoparticle serves as a fluorescence quencher. There is FRET between the embedded fluorescent dyes/QDs/metal nanoparticle and analyte-specific molecules/ligands. The fluorescence of the embedded or surface-attached dye or QD is quenched or restored when analytes bind with analyte-specific molecules/receptors. FRET-based nanoparticle sensors have been developed to detect ions, small molecules as well as cellular processes like apoptosis, using polymer and gold nanoparticles, dendrimer and QDs.

Ion sensors—Copper ion is the ion mostly studied by the FRET-based nanoparticle sensors. Some of these sensors are specifically for Cu^{2+} but others are for both Cu^{2+} and other ions. The reported sensor designs for copper ion include silica nanoparticles containing fluorescent dansylamide and a Cu^{2+} specific picolinamide subunit (72–74); latex nanoparticles containing fluorophore BODIPY and copper-chelating receptor (cyclam) (75,76); thioglycerol capped CdS QD (77) and gold nanoparticles coordinated with the fluorescent chromophore-containing pyridyl moieties through weak interactions (78). The sensitivity of the sensors was tunable by the ratio of ligand to dye (72–74). The response of the sensors was fast. For instance, there was 90% quenching of fluorescence within 1s for cyclam conjugated nanoparticle sensors (75, 76).

FRET-based sensors for copper and other ions were developed using silica nanoparticles or QD. The sensors made of silica containing polyamine chains (receptor) coupled with dansyl units (fluorophore) were selective for copper, cobalt and nickel ions (19). Pentapeptide Gly–His–Leu–Leu–Cys coated CdS QDs (2.4 ± 1.5 nm by TEM) were designed for selective detection of Cu^{2+} and Ag^{+} (79). The typical detectable range of Cu^{2+} by these sensors was in the 0.1–1000 uM and the lowest detection limit was 1nM by the latex-based sensor (75,76). However, the normal unbound copper ion level inside cells is only femtomolar. This explains why none of the copper ion nanoparticle sensors (both FRET-based sensors as well as the sensors loaded with DsRed protein described above) have been applied for intracellular studies. These sensors may be applied for cells under stressed conditions that could increase the free copper ion concentration to micromolar levels (80).

A mercury(II) FRET-based sensor was also developed with gold nanoparticles with adsorbed Rhodamine B (RB) molecules (81). A high selectivity toward Hg(II) against other metal ions

was achieved by modification of the sensor with mercaptopropionic acid, and adding a chelating ligand, 2,6-pyridinedicarboxylic acid to the test solutions. The detection limit for Hg (II) was 2.0 ppb.

Sensors for maltose—FRET-based maltose sensors have been developed using QD, maltose-binding protein (MBP) and a dye complex which forms a FRET pair with QD. In one design (82), the dye complex, β-cyclodextrin-acceptor dye conjugates, are initially bound to MBP, resulting in FRET quenching of the QD fluorescence. Added maltose displaces the dye complex, increasing the fluorescence of QD in proportion to maltose concentration. The sensors were modified to operate on a two-step FRET mechanism by labeling the MBP with another fluorescence dye, in order to overcome inherent QD donor-acceptor distance limitations. In another design (83,84), the dye complex, a ruthenium dye, is covalently linked to MBP and therefore not displaced by maltose, preventing possible error from displaceable dyes. When maltose binds with MBP, however, the interaction (distance) between the Ru complex and QD changes, leading toconcentration-dependent increase in QD fluorescence.

Apoptosis sensors—A FRET-based nanoparticle sensor for apoptosis was designed by conjugating a caspase-specific FRET-based apoptosis reagent (PhiPhiLux G1D2) to a G5 poly (amidoamine) (PAMAM) dendrimer. The sensor was conjugated with targeting moiety (folic acid) for the detection of specifc cell lines (44). The targeted apoptosis measurement by the nanosensors was demonstrated using two different cell lines: KB cell (folate receptor- positive) and UMSCC-38 cell (folate receptor-negative). When the nanoparticle sensor treated cells were exposed to the apoptosis-inducing agent staurosporine, the apoptosis was detected only in KB cells, indicating cell-specific delivery of nanoparticle sensors due to surface-conjugated targeting moieties.

3.6 SERS or LSPR sensor using metallic nanoparticles

The metallic nanoparticles (metal core nanoparticle or metal-coated polymer nanoparticle) show three unique properties: 1) fluorescence quenching; 2) SERS of surfaced-bound Raman-active molecules; 3) LSPR. The fluorescence quenching property has been utilized for FRET-based sensors as shown above (Figure 3a). SERS and LSPR have also been utilized for designing nanoparticle sensors.

The metallic SERS sensors (Figure 3b) are prepared by labeling the metallic nanoparticles with Raman active dyes that are sensitive to specific analytes such as hydrogen ion (85, 86) or large biological molecules (87). The SERS pH sensors have been developed using silver nanoparticles and gold nanoshell/silica core nanoparticles. The sensor made of silver nanoparticles (50–80 nm in diameter) functionalized with para-mercaptobenzoic acid (para-MBA) exhibited a characteristic SERS spectrum corresponding to the pH of the surrounding solution (85). The sensor was sensitive to pH changes in the range of 6–8. The nanoparticle sensors were delivered into living chinese hamster ovary cells by passive uptake for the intracellular pH measurement. The SERS spectrum showed the pH surrounding the nanoparticle to be below 6, which is consistent with the particles being located inside a lysosome (pH 5). A similar SERS pH sensor was designed based on a gold nanoshell/silica core nanoparticle coated with a layer of para-MBA (86). The nanosensor was capable of measuring pH in its local vicinity continuously, over the range of 5.80 to 7.60 pH units. The metallic LSPR sensors are prepared by conjugating the metallic nanoparticles with ligands/receptors. The extinction and scattering spectra of plasmonic nanoparticles show spectral shifts sensitive to small changes in the local refractive index. Most organic molecules have a higher refractive index than buffer solution; thus, when they bind to nanoparticles, the local refractive index increases, causing the extinction and scattering spectrum to be red shifted (35). Based on this working principle, the LSPR sensor can produce distinctive changes in LSPR upon

binding specific biological molecules to receptors on the nanoparticle surface. The LSPR sensor designs so far only include thin film on a chip or glass slide, i.e., containing large ensembles of nanoparticle sensors for biomarker proteins, rather than a single nanoparticle sensor (35).

3.7 SPIO-based MRI sensor

SPIO is a nanoparticle negative contrast agent for MRI. The SPIO sensors are prepared by conjugating the nanoparticles with ligands/receptors, which is the same design as that of metallic LSPR sensors (Figure 3c). The working principle is based on a decrease in the local T2 relaxation rates of SPIOs caused by the aggregation of SPIO particles. SPIOs conjugated with receptors/ligands have been developed for the detection of proteins and nucleic acids (88) and calcium ions (89), utilizing specific molecular interactions such as DNA–DNA, protein–protein, protein–small molecule, and enzyme reactions. For example, SPIO-based MRI sensors for Ca^{2+} were developed based on calcium-dependent interactions between the calcium-binding protein calmodulin (CaM) and a target peptide, M13 or RS20A (89). Two kinds of bioconjugated SPIOs, SPIO conjugated with CaM and SPIO with M13 or RS20A, were used for MRI monitoring of Ca ions. The calcium response of the sensors is based on selective aggregation of SPIOs in the presence of calcium. It is fully reversible but slow because the aggregation process requires considerable time (several minutes) to reach equilibrium. We note that the response time of the fluorescent Ca sensor is less than 1 ms (38). Despite such disadvantages, the MRI sensor may be useful for measurements in live, opaque specimens, as the sensing mechanism is not dependent on the separation of bound and unbound reagents and there is no problem with tissue penetration depth.

3.8 MOON sensors

MOONs (MOdulated Optical Nanoprobes) are metallically half-capped fluorescent nanoparticles. MOONs can be both magnetic (90,91), i.e., MagMOONs, or not, i.e. those used for measuring Brownian rotation (92). The magnetically induced periodic motion of the MagMOON (or random thermal motion in the case of Brownian MOONs) modulates the fluorescence signal, enabling the separation of signal from background (Figure 6). This simple procedure increases the signal-to-noise (S/N) or, strictly, signal-to-background ratios by several orders of magnitude, up to 4,000 times (90). This technique expands the breadth of applications of fluorescent nanoparticle sensors to include samples with highly scattering and/or fluorescent backgrounds or experiments with several fluorescent probes. The MOON design can be applied for any fluorescent nanoparticle sensor by adding a metal coating on one hemisphere of the nanoparticle, using either a magnetic particle or a magnetic coating metal for making MagMOONS. Moreover, the rotation behavior of the MOONs can be utilized for local viscosity measurements (93,94). A MOON sensor constructed with incorporated fluorescent pH indicator dye molecules demonstrated its capability for a simultaneous measurement of a chemical property as well as a physical property (94). Furthermore, the orientation and position of a MOON sensor can be remotely controlled by an external magnetic field, enabling spatially localized measurements (95). The MOON sensors have not yet been applied quantitatively for intracellular or in vivo measurements because MOONs so far have been developed using a micron size particle due to the size-related difficulties for efficient magnetization or high fluorescent intensity of individual sensor particle. With recent progress on nanotechnology and coating technology, such as molecular beam epitaxy, nano-meter sized MOONs are being developed (96).

SUMMARY POINTS LIST

1. The nanoparticle platform has the following advantages for intracellular and in vivo sensing: 1) physical non-invasiveness due to its small size; 2) chemical non-

invasiveness due to its inert, non-toxic matrix; 3) high accessibility of analytes because of high surface-to-volume ratio; 4) engineerability to control the loading of sensing or targeting moieties per nanoparticle and to modify the surface properties; 5) Enables multiplexing and synergistic sensor designs not possible with molecular probes; 6) Enables targeted delivery to specific cells and/or specific cell compartments; 7) Prevents sequestration into certain cell compartments; 8) In vivo they prevent uptake by the immune system; 9) In vivo they enable crossing of barriers, such as blood-brain-barrier, due to the EPR effect; 10) Cannot be pumped back out of cancer cells, thus avoiding the multidrug resistance effect.

2. Nanoparticle sensors have been constructed to detect the following: ions (H^+, Ca^{2+}, Mg^{2+}, K^+, Na^+, Cl^-, phosphate ion, Fe^{3+}, Zn^{2+}, Cu^+/Cu^{2+}, Ag^+, Hg^{2+}), small molecules (oxygen, singlet oxygen, glucose, hydrogen peroxide and maltose), hydroxyl radical, electrical field, viscosity and apoptosis. The nanoparticle sensor designs include polymer nanoparticle with incorporated fluorescent dyes; ion-correlation nanoparticle sensors; polymer nanoparticle with embedded protein; chemiluminescence sensor; FRET-based sensor; metallic nanoparticle SERS sensor; metallic nanoparticle LSPR sensor; SPIO MRI sensor; and MOON sensor.

3. Some of the above nanoparticle sensors have been successfully applied for intracellular or in vivo measurement but others were not because of insufficient sensitivity and/or selectivity. Intracellular measurement have been achieved for the following analytes: ions (H^+, Ca^{2+}, Mg^{2+}, K^+, Na^+, Cl^-) and small molecules (O_2, singlet oxygen, H_2O_2), electrical field and apoptosis. In vivo measurements were reported only for H_2O_2.

FUTURE ISSUES LIST

1. Single cell analysis has the potential for diagnosing disease at an early stage, when changes on a tissue level are not yet evident but chemical changes within cells are observable (97). Getting chemical or physical information from a single cell or a specific location within a single cell would be one of the important future applications of nanoparticle sensors.

2. The detection of multiple signals using single nanoparticle platforms would be another future application, which enables a diversity of simultaneous experiments and better controls.

3. The in vitro and in vivo application of nanoparticle sensors has been limited to a few analytes despite nanoparticle sensors designed for more diverse analytes. In order to achieve a wider application of nanoparticle sensors as well as future applications suggested in 1 & 2, the performance of nanoparticle sensors, such as signal intensity, sensitivity, and selectivity, should be improved.

4. The following may be promising future directions and opportunities for nanoparticle sensor improvements. 1) Improvement of sensing components. This will include the development of more sensitive NIR sensing dyes, more selective receptors toward analytes/targets and nanoparticle matrix/surface coatings for longer plasma circulation time. 2) Adoption of MOON-type sensor design for S/N enhancement 3) Use of remote steering by means such as magnetic or laser tweezers for spatial localization of nanoparticle sensors. 4) More enzyme based sensor stratagems, for both higher sensitivity and selectivity.

Acknowledgments

This work was supported by NIH Grants 1R01-EB-007977-01, R21/R33 CA125297 and 1R41 CA 130518-01A1 as well as NSF Grant DMR 0455330.

TERMS/DEFINITIONS LIST

Chemiluminescence	The emission of light (luminescence) without emission of heat as the result of a chemical reaction
Fluorescence	The emission of light by the molecular absorption of incident light
FRET	Förster (or Fluorescence) Resonance Energy Transfer. A distance-dependent energy transfer mechanism between two dye molecules by a nonradiative, long-range dipole-dipole coupling mechanism
Multidrug resistance	A condition enabling a disease-causing organism to resist distinct drugs or chemicals of a wide variety of structure and function targeted at eradicating the organism
Photobleaching	The photochemical destruction of a dye, resulting in bleaching of the color and the fluorescence
Ratiometric measurement	A measurement technique where a signal is measured with respect to a reference signal

ACRONYM LIST

EPR	Enhanced Permeability and Retention
LSPR	Localized Surface Plasmon Resonance
MRI	Magnetic Resonance Imaging
MOON	Modulated Optical Nanoprobe
PAA	polyacrylamide
PEBBLE	Photonic Explorer for Biomdical use with Biologically Localized Embedding
QD	Quantum Dot
ROS	Reactive Oxygen Species
SERS	Surface-Enhanced Raman Scattering
SPIO	Superparamagnetic iron oxide

LITERATURE CITED

1. Cullum BM, Vo-Dinh T. The development of optical nanosensors for biological measurements. Trends Biotechnol 2000;18:388–93. [PubMed: 10942963]
2. Haugland, RP. The Handbook: A Guide to Fluorescent Probes and Labeling Technologies. 10. Eugene: Molecular Probes Inc; 2005.
3. Buck SM, Koo YEL, Park E, Xu H, Philbert MA, Brasuel M, Kopelman R. Optochemical Nanosensor PEBBLEs: Photonic Explorers for Bioanalysis with Biologically Localized Embedding. Curr Opin Chem Biol 2004;8:540–546. [PubMed: 15450498]
4. Koo, YEL.; Agayan, R.; Philbert, MA.; Rehemtulla, A.; Ross, BD.; Kopelman, R. Photonic Explorers Based on Targeted Multifunctional Nanoplatforms: In Vitro and In Vivo Biomedical Applications. In:

Kneipp, K.; Aroca, R.; Kneipp, H.; Wentrup-Byrne, E., editors. New Approaches in Biomedical Spectroscopy. Vol. 14. New York: American Chemical Society; 2007. p. 200-18.

5. Cheong WF, Prahl SA, Welch AJ. A review of the optical properties of biological tissues. IEEE J Quantum Electron 1990;26:2166–85.
6. Delpy DT, Cope M. Quantification in tissue near-infrared spectroscopy. Phil Trans R Soc Lond B 1997;352:649–659.
7. Ntziachristos V, Bremer C, Weissleder R. Fluorescence imaging with nearinfrared light: new technological advances that enable in vivo molecular imaging. Eur Radiol 2003;13:195–208. [PubMed: 12541130]
8. Woods LA, Powell PR, Paxon TL, Ewing AG. Analysis of Mammalian Cell Cytoplasm with Electrophoresis in Nanometer Inner Diameter Capillaries. Electroanalysis 2005;17(13):1192–97. [PubMed: 17364015]
9. Brasuel M, Kopelman R, Miller TJ, Tjalkens R, Philbert MA. Fluorescent Nanosensors for Intracellular Chemical Analysis.: Decyl Methacrylate Liquid Polymer Matrix and Ion-Exchange-Based Potassium PEBBLE Sensors with Real-Time Application to Viable Rat C6 Glioma Cells. Anal Chem 2001;73 (10):2221–28. [PubMed: 11393844]
10. Koo YEL, Cao Y, Kopelman R, Koo SM, Brasuel M, Philbert MA. Real-time Measurements of Dissolved Oxygen Inside Live Cells by Ormosil (Organically Modified Silicate) Fluorescent PEBBLE Nanosensors. Anal Chem 2004;76:2498–505. [PubMed: 15117189]
11. Clark HA, Hoyer M, Parus S, Philbert MA, Kopelman R. Optochemical nanosensors and subcellular applications in living cells. Mikrochim Acta 1999;131:121–28.
12. Chan WCW, Nie SM. Quantum dot bioconjugates for ultrasensitive nonisotopic detection. Science 1998;281:2016–18. [PubMed: 9748158]
13. Akerman ME, Chan WCW, Laakkonen P, Bhatia SN, Ruoslahti R. Nanocrystal targeting in vivo. Proc Natl Acad Sci USA 2004;99(20):12617–21. [PubMed: 12235356]
14. Reddy GR, Bhojani MS, McConville P, Moody J, Moffat BA, et al. Vascular Targeted Nanoparticles for Imaging and Treatment of Brain Tumors. Clin Cancer Res 2006;12(22):6677–86. [PubMed: 17121886]
15. Kumar S, Harrison N, Richards-Kortum R, Sokolov K. Plasmonic nanosensors for imaging intracellular biomarkers in live cells. Nano Lett 2007;7(5):1338 –43. [PubMed: 17439187]
16. Tang, W. PhD thesis. Univ. Mich; Ann Arbor: 2007. Development and in vitro investigation of methylene blue-containing nanoparticle platforms for photodynamic therapy; p. 130
17. Koo YEL, Reddy GR, Bhojani M, Schneider R, Philbert MA, et al. Brain Cancer Diagnosis and Therapy with Nano-Platforms. Adv Drug Deliv Rev 2006;58:1556–77. [PubMed: 17107738]
18. Clark HA, Merritt G, Kopelman R. Novel Optical Biosensors using a Gold Colloid Monolayer Substrate. Proc SPIE (Int Soc Opt Eng) 2000;3922:138–146.
19. Montalti M, Prodi L, Zaccheroni N. Fluorescence quenching amplication in silica nanosensors for metal ions. J Mater Chem 2005;15:2810–14.
20. Montet X, Funovics M, Montet-Abou K, Weissleder R, Josephson L. Multivalent effects of RGD peptides obtained by nanoparticle display. J Med Chem 2006;49(20):6087–93. [PubMed: 17004722]
21. Kneipp K, Kneipp H, Itzkan I, Dasari RR, Feld MS. Surface-enhanced Raman scattering and biophysics. J Phys: Condens Matter 2002;14:R597–624.
22. Gobin AM, Lee MH, Halas NJ, James WD, Drezek RA, West JL. Near-infrared resonant nanoshells for combined optical imaging and photothermal cancer therapy. Nano Lett 2007;7(7):1929–34. [PubMed: 17550297]
23. Jensen TR, Malinsky MD, Haynes CL, Van Duyne RP. Nanosphere lithography: Tunable localized surface plasmon resonance spectra of silver nanoparticles. J Phys Chem B 2000;104:10549–56.
24. Clark HA, Barker SLR, Brasuel M, Miller MT, Monson E, et al. Subcellular optochemical nanobiosensors: probes encapsulated by biologically localised embedding (PEBBLEs). Sens Act B 1998;51:12–16.
25. Sasaki K, Shi ZY, Kopelman R, Masuhara H. Three-Dimensional pH Microprobing with an Optically-Manipulated Fluorescent Particle. Chem Lett 1996;25:141–142.

26. Harrell JA, Kopelman R. Biocompatible Probes Measure Intracellular Activity. Biophotonics International 2000;7:22–24.
27. Koo YEL, Fan W, Hah HJ, Kopelman R, Xu H, et al. Photonic Explorers Based on Multifunctional Nano-Platforms for Biosensing and Photodynamic Therapy. Applied Optics 2007;46(10):1924–30. [PubMed: 17356639]
28. Rhyner MN, Smith AM, Gao XH, Mao H, Yang LL, Nie SM. Quantum dots and multifunctional nanoparticles: new contrast agents for tumor imaging. Nanomedicine 2006;1(2):209–17. [PubMed: 17716110]
29. Maeda H. The enhanced permeability and retention (EPR) effect in tumor vasculature: the key role of tumor-selective macromolecular drug targeting. Advan Enzyme Regul 2001;41:189–207. [PubMed: 11384745]
30. Gao X, Cui Y, Levenson RM, Chung LWK, Nie S. In vivo cancer targeting and imaging with semiconductor quantum dots. Nat Biotechno 2004;22(8):969–76.
31. Cai W, Shin D, Chen K, Gheysens O, Cao Q, et al. In vivo targeting and imaging of tumor vasculature using arginine-glycine-aspartic acid (RGD) peptide-labeled quantum dots. Nano Lett 2006;6(4):669–76. [PubMed: 16608262]
32. Penn SG, Hey L, Natan MJ. Nanoparticles for bioanalysis. Curr Opin Chem Biol 2003;7(5):609–615. [PubMed: 14580566]
33. Kubik TK, Bogunia-Kubik K, Sugisaka M. Nanotechnology on duty in medical applications. Curr Pharm Biotechnol 2005;6(1):17–33. [PubMed: 15727553]
34. Fischer NO, Tarasow TM, Tok JBH. Heightened sense for sensing: recent advances in pathogen immunoassay sensing platforms. Analyst 2007;132(3):187–91. [PubMed: 17325749]
35. Anker JN, Hall WP, Lyandres O, Shah NC, Zhao J, Van Duyne RP. Biosensing with plasmonic nanosensors. Nat Mater 2008;7(6):442–53. [PubMed: 18497851]
36. Kopelman R, Tan W. Near-Field Optics: Imaging Single Molecules. Science 1993;262:1382–1384. [PubMed: 17736816]
37. Park EJ, Brasuel M, Behrend C, Philbert MA, Kopelman R. Ratiometric optical PEBBLE nanosensors for real-time magnesium ion concentrations inside viable cells. Anal Chem 2003;75(15):3784–91. [PubMed: 14572044]
38. Clark HA, Hoyer M, Philbert MA, Kopelman R. Optical nanosensors for chemical analysis inside single living cells. 1 Fabrication, characterization, and methods for intracellular delivery of PEBBLE sensors. Anal Chem 1999;71(21):4831–36. [PubMed: 10565274]
39. Sumner JP, Aylott JW, Monson E, Kopelman R. A Fluorescent PEBBLE Nanosensor for Intracellular Free Zinc. Analyst 2002;127:11–16. [PubMed: 11827375]
40. Sumner JP, Westerberg N, Stoddard AK, Fierke CA, Kopelman R. Cu^{+} and Cu^{2+} sensitive PEBBLE fluorescent nanosensors using Ds Red as the recognition element. Sens Act B 2005;113(2):760–67.
41. Sumner JP, Kopelman R. Alexa Fluor 488 as an iron sensing molecule and its application in PEBBLE nanosensors. Analyst 2005;130(4):528–33. [PubMed: 15776163]
42. Cao Y, Koo YL, Kopelman R. Poly (Decyl Methacrylate)-based Fluorescent PEBBLE Swarm Nanosensors for measuring dissolved oxygen in biosamples. Analyst 2004;129:745–50. [PubMed: 15284919]
43. Horvath T, Monson E, Sumner J, Xu H, Kopelman R. Use of Steady-State Fluorescence Anisotropy with PEBBLE Nanosensors for Chemical Analysis. Proc SPIE (International Society of Photonic Engineering) 2002;4626:482–92.
44. Myc A, Majoros IJ, Thomas TP, Baker JR. Dendrimer-based targeted delivery of an apoptotic sensor in cancer cells. Biomacromolecules 2007;8(1):13–1. [PubMed: 17206782]
45. Almdal K, Sun HH, Poulsen AK, Arleth L, Jakobsen I, et al. Fluorescent gel particles in the nanometer range for detection of metabolites in living cells. Polym Adv Technol 2006;17:790–93.
46. Brown JQ, McShane MJ. Core-referenced ratiometric fluorescent potassium ion sensors using self-assembled ultrathin films on europium nanoparticles. IEEE Sensors J 2005;5(6):1197–205.
47. King M, Kopelman R. Development of a hydroxyl radical ratiometric nanoprobe. Sens Act B 2003;90:76–81.

48. Cao Y, Koo YEL, Koo S, Kopelman R. Ratiometric singlet oxygen nano-optodes and their use for monitoring photodynamic therapy nanoplatforms. Photochem Photobiol 2005;81(6):1489–98. [PubMed: 16107183]
49. Xu H, Aylott JW, Kopelman R, Miller TJ, Philbert MA. A real-time ratiometric method for the determination of molecular oxygen inside living cells using sol-gel-based spherical optical nanosensors with applications to rat C6 glioma. Anal Chem 2001;73:4124–33. [PubMed: 11569801]
50. Guice KB, Caldorera ME, McShane MJ. Nanoscale internally referenced oxygen sensors produced from self-assembled nanofilms on fluorescent nanoparticles. J Biomed Opt 2005;10(6) 10:064031–1–10.
51. Cheng ZL, Aspinwall CA. Nanometre-sized molecular oxygen sensors prepared from polymer stabilized phospholipid vesicles. Analyst 2006;131(2):236–43. [PubMed: 16440088]
52. Schmälzlin E, van Dongen JT, Klimant I, Marmodée B, Steup M, et al. An optical multifrequency phase-modulation method using microbeads for measuring intracellular oxygen concentrations in plants. Biophys J 2005;89(2):1339–45. [PubMed: 16049223]
53. Schmälzlin E, Walz B, Klimant I, Schewe B, Löhmannsröben HG. Monitoring hormone-induced oxygen consumption in the salivary glands of the blowfly, Calliphora vicina, byuse of luminescent microbeads. Sens Act B 2006;119(1):251–54.
54. Kim, G. PhD thesis. Univ. Mich; Ann Arbor: 2008. Development of Nanoparticle Based Tools for Reactive Oxygen Species and Related Biomedical Applications; p. 151
55. Tyner KM, Kopelman R, Philbert MA. Nanosized voltmeter" enables cellular-wide electric field mapping. Biophys J 2007;93(4):1163–74. [PubMed: 17513359]
56. Martin-Orozco N, Touret N, Zaharik ML, Park E, Kopelman R, et al. Visualization of Vacuolar Acidification-induced Transcription of Genes of Pathogens inside Macrophages. Mol Biol Cell 2006;17(1):498–510. [PubMed: 16251362]
57. Vescovi EG, Soncini FC, Groisman EA. Mg^{2+} as an extracellular signal: Environmental regulation of Salmonella virulence. Cell 1996;84(1):165–74. [PubMed: 8548821]
58. Brasuel M, Kopelman R, Kasman I, Miller TJ, Philbert MA. Ion Concentrations in Live Cells from Highly Selective Ion Correlations Fluorescent Nano-Sensors for Sodium. Proc IEEE Sensors 2002;1:288–92.
59. Brasuel MG, Miller TJ, Kopelman R, Philbert MA. Liquid Polymer Nano-PEBBLES for Cl- Analysis and Biological Applications. Analyst 2003;128(10):1262–67. [PubMed: 14667163]
60. Dubach JM, Harjes DI, Clark HA. Fluorescent Ion-Selective Nanosensors for Intracellular Analysis with Improved Lifetime and Size. Nano Lett 2007;7(6):1827–31. [PubMed: 17497824]
61. Dubach JM, Harjes DI, Clark HA. Ion-Selective Nano-optodes Incorporating Quantum Dots. J Am Chem Soc 2007;129:8418–19. [PubMed: 17567136]
62. Ruedas-Rama MJ, Hall EAH. K^{+}-selective nanospheres: maximizing response range and minimizing response time. Analyst 2007;131(12):1282–91. [PubMed: 17124535]
63. Bühlmann P, Pretsch E, Bakker E. Carrier-based ion-selective electrodes and bulk optodes, 2. Ionophores for potentiometric and optical sensors. Chem Rev 1998;98(4):1593–687. [PubMed: 11848943]
64. Shortreed MR, Bakker E, Kopelman R. Miniature sodium selective ion-exchange optode with fluorescent pH chromoionophores and tunable dynamic range. Anal Chem 1996;68:2656–62. [PubMed: 8694263]
65. Shortreed MR, Barker SLR, Kopelman R. Anion-Selective Liquid-Polymer Optodes with Fluorescent pH Chromoionophores, Tunable Dynamic Range and Diffusion Enhanced Lifetimes. Sens Act B 1996;35:217–21.
66. Shortreed MR, Dourado S, Kopelman R. Development of a Fluorescent Optical Potassium-Selective Ion Sensor with Ratiometric Response for Intracellular Applications. Sens Act B 1997;38:8–12.
67. Lee D, Khaja S, Velasquez-Castano JC, Dasari M, Sun C, et al. In vivo imaging of hydrogen peroxide with chemiluminescent nanoparticles. Nat Mater 2007;6(10):765–69. [PubMed: 17704780]
68. Sun HH, Scharff-Poulsen AM, Gu H, Jakobsen I, Kossmann JM, et al. Phosphate sensing by fluorescent reporter proteins embedded in polyacrylamide nanoparticles. ACS Nano 2008;2(1):19–24. [PubMed: 19206543]

69. Xu H, Aylott JW, Kopelman R. Fluorescent nano-PEBBLE sensors designed for intracellular glucose imaging. Analyst 2002;127(11):1471–77. [PubMed: 12475037]
70. Poulsen AK, Scharff-Poulsen AM, Olsen LF. Horseradish peroxidase embedded in polyacrylamide nanoparticles enables optical detection of reactive oxygen species. Anal Biochem 2007;366(1):29–36. [PubMed: 17498639]
71. Kim SH, Kim B, Yadavalli VK, Pishko MV. Encapsulation of enzyme within polymer spheres to create optical nanosensors for oxidative stress. Anal Chem 2005;77(21):6828–33. [PubMed: 16255579]
72. Brasola E, Mancin F, Rampazzo E, Tecilla P, Tonellato U. A fluorescence nanosensor for Cu^{2+} on silica particles. Chem Commun 2003;24:3026–27.
73. Rampazzo E, Brasola E, Marcuz S, Mancin F, Tecilla P, Tonellato U. Surface modification of silica nanoparticles: a new strategy for the realization of self-organized fluorescent chemosensors. J Mater Chem 2005;15:2687–96.
74. Arduini M, Marcuz S, Montolli M, Rampazzo E, Mancin F, et al. Turning fluorescent dyes into Cu (II) nanosensors. Langmuir 2005;21(20):9314–21. [PubMed: 16171367]
75. Méallet-Renault R, Pansu R, Amigoni-Gerbier S, Larpent C. Metal-chelating nanoparticles as selective fluorescent sensor for Cu^{2+} Chem Commun 2004;20:2344–45.
76. Méallet-Renault R, Hérault A, Vachon JJ, Pansu RB, Amigoni-Gerbier S, Larpent C. Fluorescent nanoparticles as selective Cu(II) sensors. Photochem Photobiol Sci 2006;5(3):300–10. [PubMed: 16520865]
77. Chen YF, Rosenzweig Z. Luminescent CdS quantum dots as selective ion probes. Anal Chem 2002;74 (19):5132–38. [PubMed: 12380840]
78. He X, Liu H, Li Y, Wang S, Li Y, et al. Nanoparticle-based fluorometric and colorimetric sensing of copper(II) ions. Advan Mat 2005;17(23):2811–15.
79. Gattas-Asfura KM, Leblanc RM. Peptide-coated CdS quantum dots for the optical detection of copper (II) and silver(I). Chem Commun 2003;21:2684–85.
80. Bush AI. Metals and neuroscience. Curr Opin Chem Biol 2000;4(2):184–91. [PubMed: 10742195]
81. Huang CC, Chang HT. Selective Gold-Nanoparticle-Based "Turn-On" Fluorescent Sensors for Detection of Mercury(II) in Aqueous Solution. Anal Chem 2006;78:8332–38. [PubMed: 17165824]
82. Medintz IL, Clapp AR, Mattoussi H, Goldman ER, Fisher B, Mauro JM. Self-assembled nanoscale biosensors based on quantum dot FRET donors. Nat Mater 2003;2(9):630–38. [PubMed: 12942071]
83. Sandros MG, Gao D, Benson DE. A modular nanoparticle-based system for reagentless small molecule biosensing. J Am Chem Soc 2005;127(35):12198–99. [PubMed: 16131178]
84. Sandros MG, Shete V, Benson DE. Selective, reversible, regentless maltose biosensing with core-shell semiconducting nanoparticles. Analyst 2006;131(2):229–35. [PubMed: 16440087]
85. Talley CE, Jusinski L, Hollars CW, Lane SM, Huser T. Intracellular pH sensors Based on Surface-Enhanced Raman Scattering. Anal Chem 2004;76:7064–68. [PubMed: 15571360]
86. Bishnoi SW, Rozell CJ, Levin CS, Gheith MK, Johnson BR, et al. All-optical nanoscale pH meter. Nano Lett 2006;6(8):1687–92. [PubMed: 16895357]
87. Cao YC, Jin R, Mirkin CA. Nanoparticles with Raman spectroscopic fingerprints for DNA and RNA detection. Science 2002;297:1536–40. [PubMed: 12202825]
88. Perez JM, Josephson L, O'Loughlin T, Hogemann D, Weissleder R. Magnetic relaxation switches capable of sensing molecular interactions. Nat Biotechnol 2002;20:816–20. [PubMed: 12134166]
89. Atanasijevic T, Shusteff M, Fam P, Jasanoff A. Calcium-sensitive MRI contrast agents based on superparamagnetic iron oxide nanoparticles and calmodulin. Proc Natl Acad Sci USA 2006;103:14707–12. [PubMed: 17003117]
90. Anker JN, Kopelman R. Magnetically modulated optical nanoprobes. Appl Phys Lett 2003;82(7): 1102–4.
91. Anker JN, Behrend C, Kopelman R. Aspherical Magnetically Modulated Optical Nanoprobes (MagMOONs). J Appl Phys 2003;93(10):6698–700.
92. Behrend CJ, Anker JN, Kopelman R. Brownian Modulated Optical Nanoprobes. Appl Phys Lett 2004;84(1):154–56.

93. Behrend CJ, Anker JN, McNaughton BH, Kopelman R. Microrheology with modulated optical nanoprobes (MOONs). J Mag Magn Mater 2005;293(1):663–70.

94. McNaughton BH, Agayan RR, Wang JX, Kopelman R. Physiochemical microparticle sensors based on nonlinear magnetic oscillations. Sens Act B 2007;121(1):330–40.

95. Anker JN, Koo YE, Kopelman R. Magnetically controlled sensor swarms. Sens Act B 2007;121(1): 83–92.

96. McNaughton, BH. PhD thesis. Univ. Mich; Ann Arbor: 2007. Magnetic micro and nano nonlinear oscillators with applications to the dynamic detection of a single bacterium and to physical and chemical sensing; p. 113

97. Soper SA, Brown K, Ellington A, Frazier B, Garcia-Manero G, et al. Point-of-care biosensor systems for cancer diagnostics/prognostics. Biosen & Bioele 2006;21(10):1932–42.

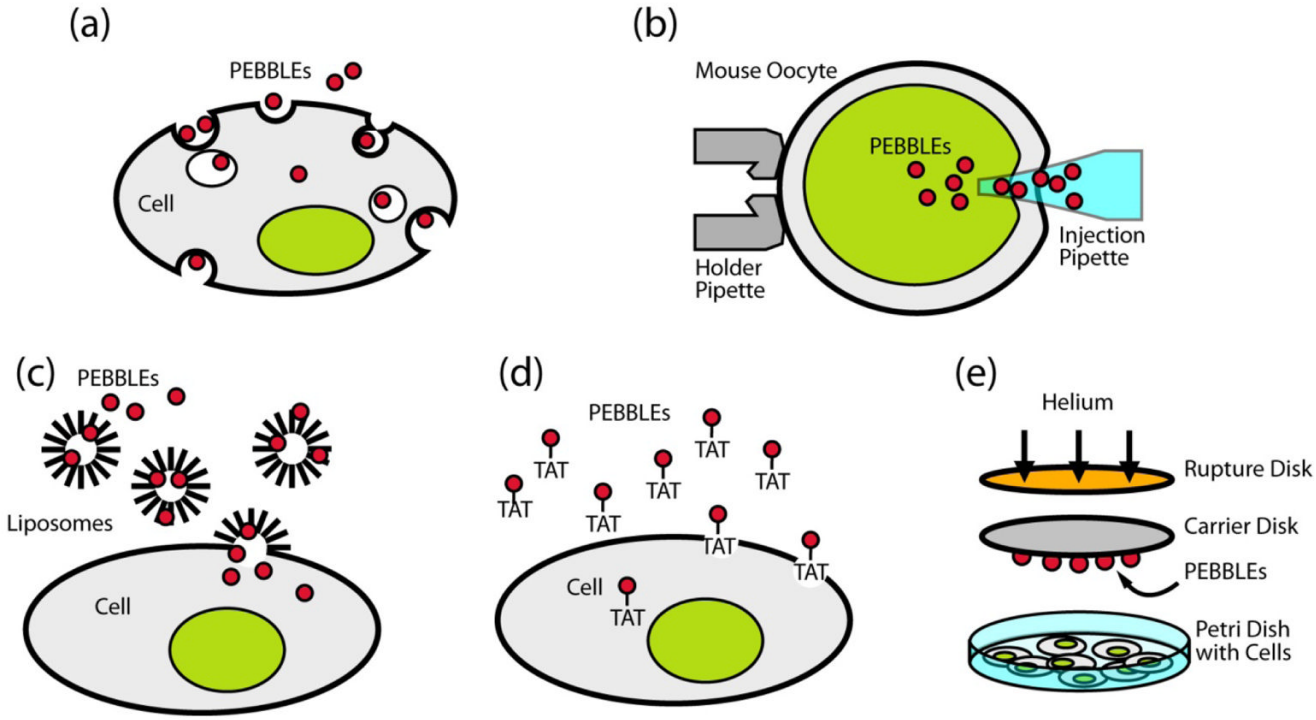

Figure 1. Nanoparticle delivery methods into single cells for bioanalysis

(a) Endocytosis (non-specific or receptor-mediated); (b) Picoinjection; (c) Liposomal delivery; (d) Membrane penetration peptide (TAT); (e) Gene gun

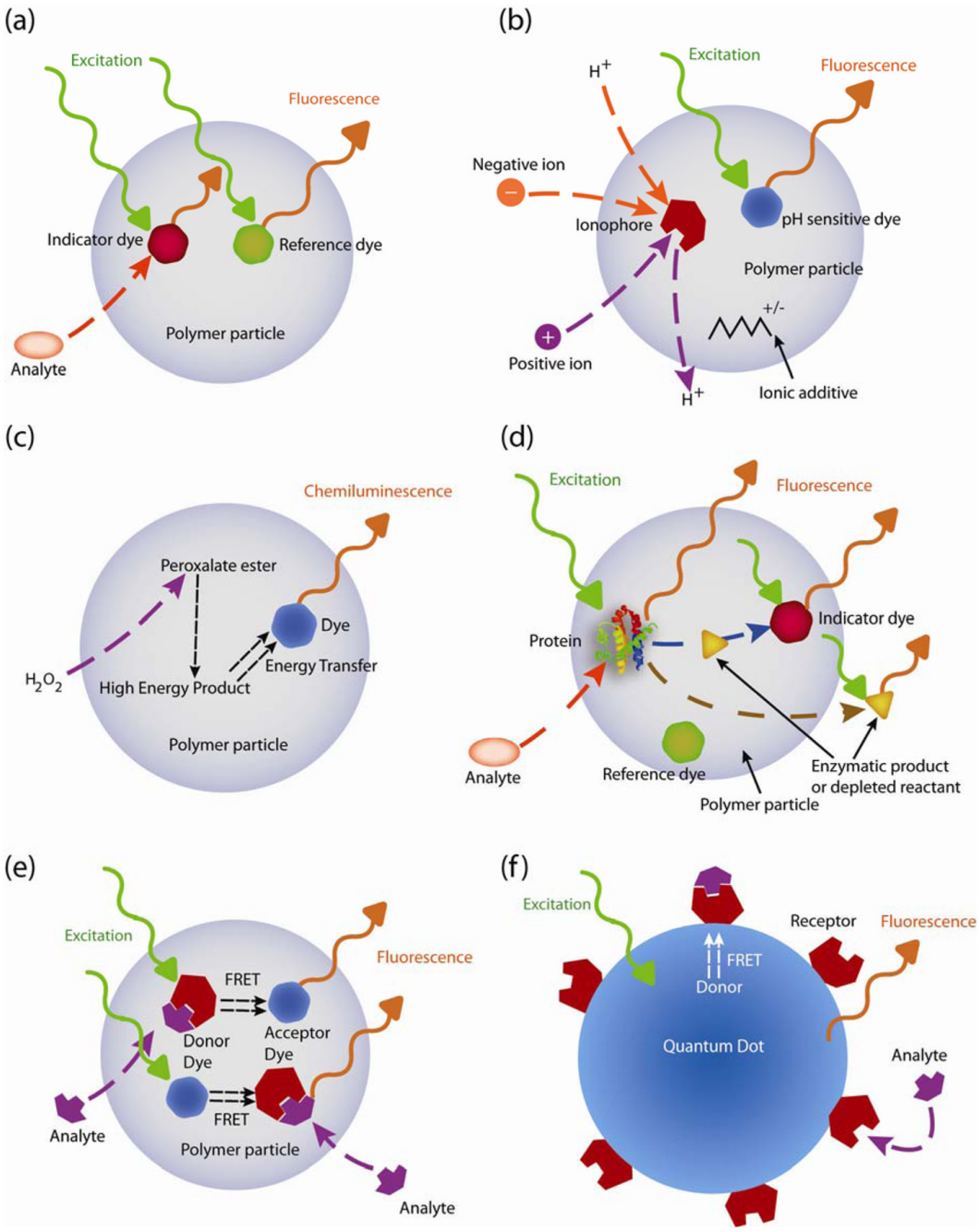

Figure 2. Schematic diagrams of various designs of luminescent nanoparticle sensors

(a) Polymer nanoparticle sensor with fluorescent indicator dyes; (b) Ion-correlation nanoparticle sensor; (c) Chemiluminescence nanoparticle sensor; (d) Polymer nanoparticle sensor with encapsulated protein; (e) FRET-based polymer nanoparticle sensor; (f) FRET-based QD sensor

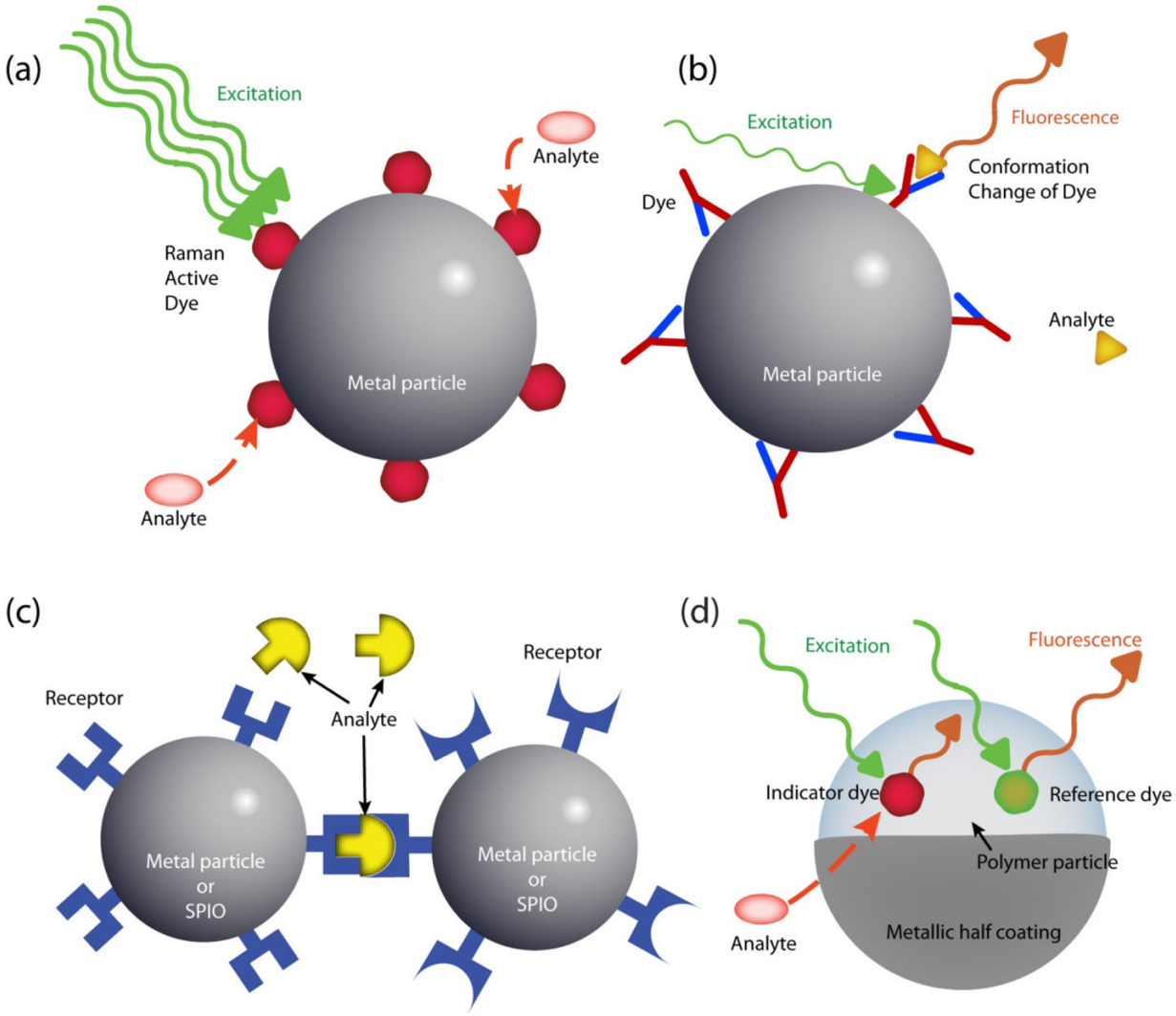

Figure 3. Schematic diagrams of sensor designs based on metallic nanoparticle and/or SPIO

(a) Fluorescent sensor: metallic nanoparticle conjugated with fluorescent receptors; (b) SERS sensor: metallic nanoparticle with surface-coated Raman active indicator dye; (c) LSPR sensor or MRI sensor: metallic nanoparticles or SPIOs, conjugated with receptors; (d) MOON sensor. Note: The LSPR or MRI sensor detects the signal change from the aggregation status of the sensors, requiring a multiple number of the particles.

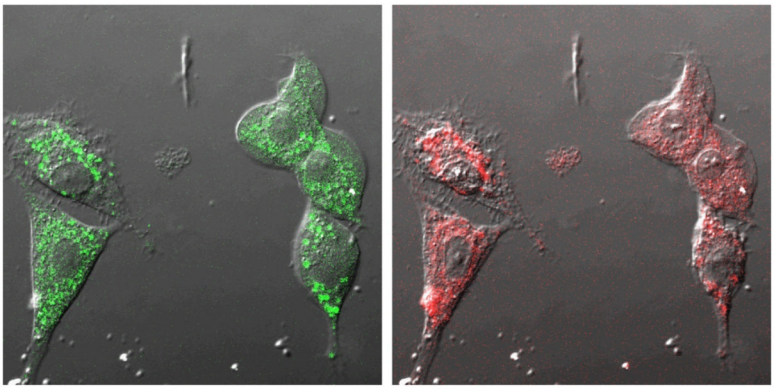

Figure 4.

Confocal images of rat C6 glioma cells loaded with sol gel PEBBLEs by gene-gun injection. Nomarski illumination image overlaid with Oregon Green fluorescence (reference, *left*) and $[Ru(dpp)_3]^{2+}$ fluorescence (oxygen indicator, *right*) of the same ratiometric PEBBLEs inside cells. (Adapted from reference [49], with permission from ACS)

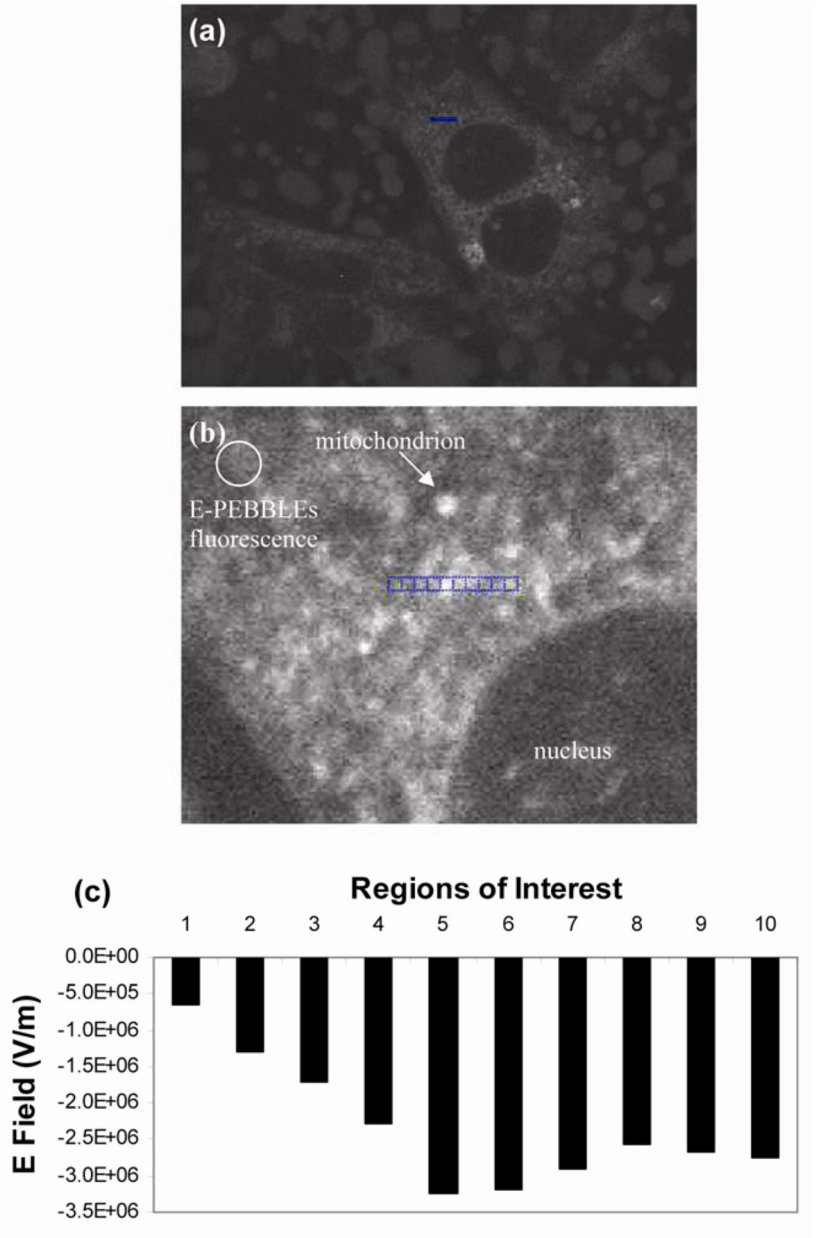

Figure 5. E-PEBBLEs can measure E fields in both cytosolic and membrane regions of living cells

(a) Astrocytes incubated with E-PEBBLEs. The middle cell contains the region analyzed (blue scale bar, 4.5 microns). (b) An enlarged image of the cellular region analyzed (both membrane and cytosolic regions). An arrow points out a representative mitochondrion. The circular region contains diffuse fluorescence arising from the E- PEBBLEs. The blue pixels indicate the regions analyzed. The regions are numbered 1–10 from left to right. Region 5 contains a mitochondrion (brightly fluorescent region), whereas regions 6–10 cross over other mitochondrial regions. The brightness and contrast of this image has been adjusted to 68% and 83% (from 50%, Microsoft Publisher), respectively, for added clarity. (c) A graph showing the E field for the regions analyzed before the addition of CCCP. The highest E field is seen in region 5. (Adapted from reference [55], with permission from The Biophysical Society)

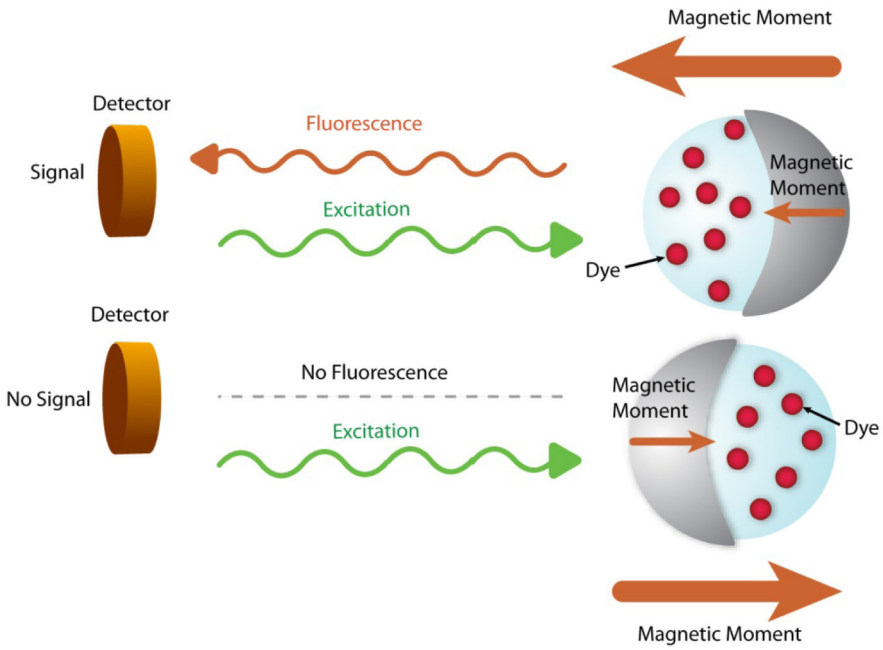

Figure 6.
Background free measurement by MagMOON. An external magnetic field orients the MagMOON, causing its fluorescent excitation and observed emission to blink on and off as it rotates. We note that the background fluorescence does not blink.

Table 1

Dissolved oxygen nanoparticle sensors

Matrix	Size	Oxygen indicator	Optical signal	Q_{DO}	References
Silica	20–300nm	Ru(II)- tris(4,7-diphenyl-1,10-phenanthroline) dichloride	Fluorescence intensity	80%	(49)
			Fluorescence Anisotropy	N/A	(43)
Ormosil	120nm	Pt(II) octaethylporphine ketone	Fluorescence intensity	97%	(10)
Ormosil	120nm	Pt(II) octaethylporphine	Fluorescence intensity	97%	(10)
PDMA	150–250nm	Pt(II) octaethylporphine ketone	Fluorescence intensity	97.5%	(42)
Commercial fluorophore coated with polyelectrolyte layers	100nm	Ru(II)-tris(4,7-diphenyl-1,10-phenanthroline) dichloride	Fluorescence intensity	60%	(50)
Polymerized liposome	150nm	Ru(II)- tris(4,7-diphenyl-1,10-phenanthroline) dichloride	Fluorescence intensity	76%	(51)
polystyrene	300nm–1μm	Pt(II)-tetra-pentafluorophenyl-porphyrin	Fluorescence lifetime	N/A	(52,53)